

A biophysical limit for quorum sensing in biofilms

Avaneesh V. Narla^a, David Borenstein^b, and Ned S. Wingreen^{c,d,*}

^aDepartment of Physics, University of California, San Diego, 9500 Gilman Drive, La Jolla, CA 92092; ^bCharity Navigator; ^cDepartment of Molecular Biology, Princeton University, Princeton, NJ 08544; ^dLewis-Sigler Institute for Integrative Genomics, Princeton University, Princeton, NJ 08544

This manuscript was compiled on November 1, 2020

Bacteria grow on surfaces in complex immobile communities known as biofilms, which are composed of cells embedded in an extracellular matrix. Within biofilms, bacteria often interact with members of their own species, and cooperate or compete with members of other species via quorum sensing (QS). QS is a process by which microbes produce, secrete, and subsequently detect small molecules called autoinducers (AIs) to assess their local population density. We explore the competitive advantage of QS through agent-based simulations of a spatial model in which colony expansion via extracellular matrix production provides greater access to a limiting diffusible nutrient. We note a significant difference in results based on whether AI production is constitutive or limited by nutrient availability: If AI production is constitutive, simple QS-based matrix-production strategies can be far superior to any fixed strategy. However, if AI production is limited by nutrient availability, QS-based strategies fail to provide a significant advantage over fixed strategies. To explain this dichotomy, we derive a novel biophysical limit for the dynamic range of nutrient-limited AI concentrations in biofilms. This range is remarkably small (less than 10-fold) for the realistic case in which a growth-limiting diffusible nutrient is taken up within a narrow active growth layer. This biophysical limit implies that for QS to be most effective in biofilms, AI production should be a protected function not directly tied to metabolism.

quorum sensing | biofilms | agent-based modeling | nutrient-limited communication

Many species of bacteria form immobile communities of densely packed cells called biofilms (1). Cells in biofilms are embedded in an extracellular matrix composed of biopolymers, including polysaccharides, proteins, nucleic acids, and lipids. Advantages provided by the matrix include adhering cells to each other and to a substrate, creating a protective barrier against chemicals and predators, and facilitating horizontal gene transfer. Formation of biofilms both relies on and promotes cell-cell chemical communication – a process known as quorum sensing (QS). QS depends on the secretion and detection of small, diffusible molecules known as autoinducers (AIs), whose concentration increases with increasing cell density. QS has been demonstrated to be critical to proper biofilm formation (2–7). For example, *Pseudomonas aeruginosa* mutants that do not synthesize AIs terminate biofilm formation at an early stage (8).

How might cells benefit from QS regulation of matrix production? In simple models of biofilms that incorporate realistic reaction-diffusion effects, Xavier et al. (9) found that matrix production allows cells to push descendants outwards from a surface into a more O₂-rich environment. Consequently, they found that matrix production provides a strong competitive advantage to cell lineages by suffocating neighboring non-producing cells (9). Building upon this work, Nadell et al. (10) showed that strategies that employ QS to deactivate matrix production in mature biofilms can yield a further ad-

vantage by redirecting resources into reproduction, and this scenario has been replicated and further developed (11–14). Notably, all these models assume constitutive AI production with no dependence on nutrient availability (10–14). Yet in many cases AI production relies on central metabolic compounds. For example, a substrate for synthesis of ubiquitous acyl-HSL AIs is produced by one-carbon metabolism, which is highly dependent on nutrient availability (15–17). Thus, we sought to understand whether QS regulation of matrix production is still advantageous if AI production depends on cells' access to nutrients.

To this end, we simulated competitions among biofilm-forming cells, comparing strategies that employ QS with strategies that do not. While QS cells that constitutively produce AI could outcompete all fixed strategies, we found, surprisingly, that nutrient-dependent QS provided essentially no advantage over non-QS cells. We trace this result to a novel biophysical limit on the dynamic range of nutrient-limited AI concentrations.

Results

Agent-based Model. For simplicity and ease of visualization, we performed simulations with agent-based models (ABMs) on a two-dimensional square lattice (Fig. 1A). ABMs represent a system as an ensemble of autonomous agents which interact with one another according to predefined behaviors (18). In our simulations, a square can be occupied by a cell, an equivalent volume of matrix, or be unoccupied. Cells start at the bottom of the simulation domain, which is taken as the substrate to

Significance Statement

Biofilms are a ubiquitous form of bacterial community. Since biofilm growth is generally limited by access to diffusible nutrients, bacteria compete by producing matrix which allows rapid colony expansion towards the nutrient source. Within biofilms, bacteria communicate via chemical signals in a process called quorum sensing (QS). It has been suggested that QS allows bacteria to tune matrix production, e.g. to first outgrow competitors but then devote more resources to population growth. However, if signal production is nutrient-limited, then the nutrient-deficient interior of a biofilm cannot contribute to QS. Indeed, we report a novel biophysical limit on the efficacy of QS under nutrient limitation, which suggests that such communication must be a prized function that is not metabolically slaved.

A.V.N. and N.S.W. designed research; A.V.N. and N.S.W. performed research; A.V.N., D.B., and N.S.W. developed computational tools; A.V.N. and N.S.W. analyzed data; and A.V.N. and N.S.W. wrote the paper.

The authors declare no conflict of interest.

*To whom correspondence should be addressed. E-mail: wingreen@princeton.edu

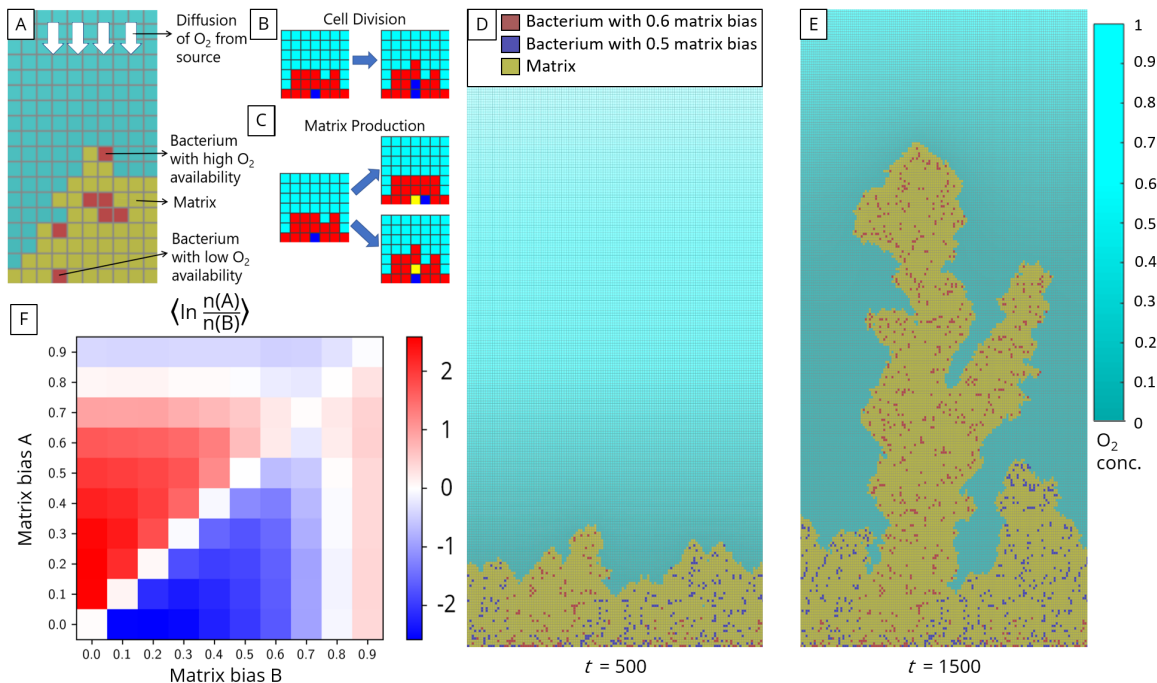


Fig. 1. Simulated competitions of matrix-producing biofilms that grow on a submerged surface toward an O₂ source. For details please see *Materials and Methods* and *SI Appendix*. (A) All simulations are performed on a 2D square lattice of width 128 sites and height 256 sites. Red squares are bacterial cells, yellow squares are extracellular matrix, and cyan squares are unoccupied. White arrows indicate diffusion of O₂ from above. (B) Schematic of cell division and matrix production, shown for a blue cell surrounded by red cells. Cell division results in an identical cell being placed in an adjacent site. If no adjacent site is available, cells are shoved out of the way to make room for the new cell. Similarly, matrix production results in filling of an adjacent site with matrix. (C) Snapshot of a pairwise competition after 500 simulation timesteps. Red cells have matrix bias of 0.6 while blue cells have matrix bias of 0.5. Shade of cyan squares indicates normalized O₂ concentration (normalized by the highest O₂ concentration recorded for the entire simulation). (D) Snapshot of the same competition in C after 1,500 timesteps. (E) Mean of the natural logarithm of the final ratio of number of cells with matrix bias A to number of cells with matrix bias B. Between 75 and 350 simulations were performed for each competition.

55 which the biofilm adheres. Cells may reproduce and form
 56 identical copies of themselves or produce matrix (see Fig. 1B
 57 and C). Matrix itself performs no actions, but fills space.

58 Both reproduction and matrix production may require shov-
 59 ing to make an adjacent site available. Shoving is performed
 60 by first choosing a nearest vacant site and a shortest path to
 61 the chosen vacant site (both of which may not be unique);
 62 then, all occupants of the squares in the path are displaced
 63 along the path towards the vacant site. In our simulations,
 64 cells are assumed to be immotile and thus only move when
 65 shoved. Thus, the biofilm, composed of cells and the matrix
 66 they produce, increases in biomass and grows upward. Each
 67 simulation ends when 50% of the lattice sites become occupied
 68 or a cell reaches the top of the simulation domain.

69 Biomass production in biofilms requires nutrients. For
 70 example, aerobic biofilms depend on oxygen (O₂) which usually
 71 diffuses in from a source located far away (9, 19–21). In our
 72 simulations, we consider a single limiting nutrient, taken to be
 73 O₂, which diffuses from the top boundary of the simulation
 74 domain at a constant flux, mimicking a distant source (*SI*
 75 *Appendix*). We assume strong O₂ uptake by bacterial cells
 76 to allow for a well-defined surface-growth layer within our
 77 small simulation domain. Since the timescale for the O₂
 78 concentration to come to a quasi-steady state (~20s for our
 79 simulation domain) is much shorter than the timescale of
 80 biomass production (~1 hour), we assume a separation of the
 81 two timescales.

82 Biomass production in the simulated biofilm is limited by

O₂ uptake, which we assume to be proportional to local O₂
 concentration. Thus, if the uptake of O₂ is rapid, only cells in
 the upper layers of the biofilm have access to O₂ and produce
 biomass. We define the fraction of O₂ uptake used for matrix
 production to be the *matrix bias*. For the same amount of O₂
 taken up, a bacterium can produce a much greater volume of
 matrix than of new cells (we take the cost of matrix production
 to be 1/14 of the cost of reproduction on a per volume basis
 (22)).

Bacterial Competitions. To estimate the optimal matrix bias
 for bacteria in our model, we performed pairwise competitions
 between different matrix-bias strategies (Fig. 1D-F). We com-
 pared the cell counts of the different strategies at the end of the
 simulations, and found that a matrix bias of approximately 0.7
 (Fig. 1F) performs better on average than any other constant
 matrix bias. Although the value of this “optimal” matrix bias
 depends on the simulation conditions (e.g., for a lower propor-
 tional cost of matrix, a higher matrix bias would be optimal),
 the non-zero value indicates that matrix production affords
 bacteria a fitness advantage in the presence of competition (a
 similar conclusion was reached by Xavier et al. (9) who used
 a realistic geometry for their simulations; Xavier et al. also
 utilized two limiting reactants, oxygen and a carbon substrate,
 and assumed Michaelis-Menten kinetics for their uptake by
 the bacteria (9, 23)).

As seen in Fig. 1E, after some time the cells of one strategy
 may overshadow their competitors and subsequently consume

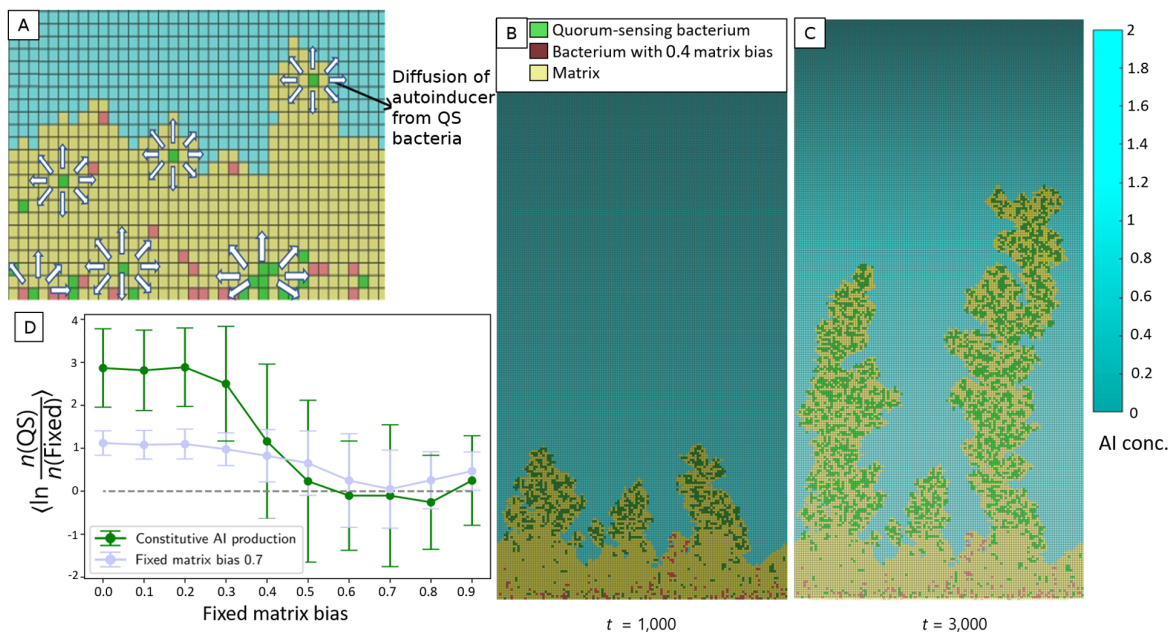


Fig. 2. Simulated biofilm competitions between QS and non-QS cells. (A) QS cells shown in green produce autoinducer (AI) at a constant rate; arrows indicate AI diffusion. QS cells adjust their matrix bias based on local AI concentration. (B) Snapshot of a pairwise competition after 1,000 simulation timesteps. Green QS cells produce and detect AI and adjust their matrix bias from $b_{\max} = 0.9$ at zero AI down to $b_{\min} = 0.1$ at high AI (see Eq. 1). Non-QS cells (red) do not produce AI and have a fixed matrix bias of 0.4. O_2 diffuses from above as in Fig. 1, but color shade now indicates local AI concentration (in arbitrary units as described in the *SI Appendix*). (C) Snapshot of the same competition in B after 3,000 timesteps. (D) Mean of the natural logarithm of the final ratio of number of QS cells to number of fixed-matrix-bias cells (green curve). For comparison, the results of the pairwise competitions for the optimal fixed-strategy matrix bias of 0.7 are also shown. The error bars indicate standard deviations of log ratios. 42-65 simulations were performed for each competition.

the entire flux of O_2 . Because after this time there is no further competition between strains, continued production of matrix by the “winning” strain would not increase access to O_2 , and could be viewed as a waste of resources. Thus switching to a low matrix bias strategy in the absence of competition could allow bacteria to increase their integrated reproductive rate. Following (9, 10), we hypothesized that bacteria could use intercellular communication (such as QS) to switch from a high matrix bias to a low matrix bias after having gained a monopoly over the nutrient and so perform better than any strategy with a fixed matrix bias.

To test this hypothesis, we incorporated QS into our simulations (Fig. 2). We performed pairwise competitions between strategies that employed QS and strategies that did not. We assumed QS bacteria constitutively produce diffusible AI, and detect local AI concentration to regulate their matrix bias. We modeled the matrix bias, b , of the QS bacteria as a Hill function,

$$b([AI]) = b_{\min} + (b_{\max} - b_{\min}) \frac{[AI]^h}{K^h + [AI]^h}, \quad [1]$$

where K is the AI concentration at which b attains the value $\frac{1}{2}(b_{\min} + b_{\max})$, halfway between its minimum and maximum. We chose $h = 10$ to yield a near switch-like response to AI. Indeed, by varying b_{\min} , b_{\max} , and K we found multiple QS strategies that performed better than all fixed-matrix-bias strategies. A similar conclusion was reached by Nadell et al. (10) by employing a framework similar to Xavier et al. (9) and assuming constitutive AI production.

But what if AI production is nutrient-dependent, i.e. is QS still beneficial in a nutrient-limited environment? To investigate this question, we let AI production depend linearly on local O_2 concentration. As shown in Fig. 3, we performed pairwise competitions between fixed-matrix-bias cells and QS cells, now with nutrient-dependent AI production. Strikingly, we found that nutrient-limited QS *did not* provide a substantial competitive benefit. Specifically, nutrient-limited QS strategies had to be highly fine-tuned to ever perform better overall than fixed strategies, and at best they did not perform nearly as well as QS strategies with constitutive AI production. Notably, though the nutrient-limited QS strategies initially switched from high matrix bias to low matrix bias, the cells later switched back to a high matrix bias and thus failed to capitalize on the lack of competition.

What is it that prevents nutrient-limited QS bacteria that have achieved dominance from switching to a low matrix bias? We observed that only the cells at the edge of the biofilm produce substantial amounts of AI (as O_2 penetration into the biofilm was designed to be low) and so the total AI production remains nearly constant. Thus, despite the increasing total population of QS bacteria, the AI concentration at the growing front of the biofilm does not increase over time. (Note that we assume a slow decay of AI, yielding a decay length of $\sim 100\mu\text{m}$, to avoid artifacts associated with the finite simulation domain size.) As a result, the nutrient-limited QS bacteria are not able to distinguish between being at the edge of a large “successful” biofilm, and being part of the initial seeding density of bacteria, still in competition with other species. This contrasts with

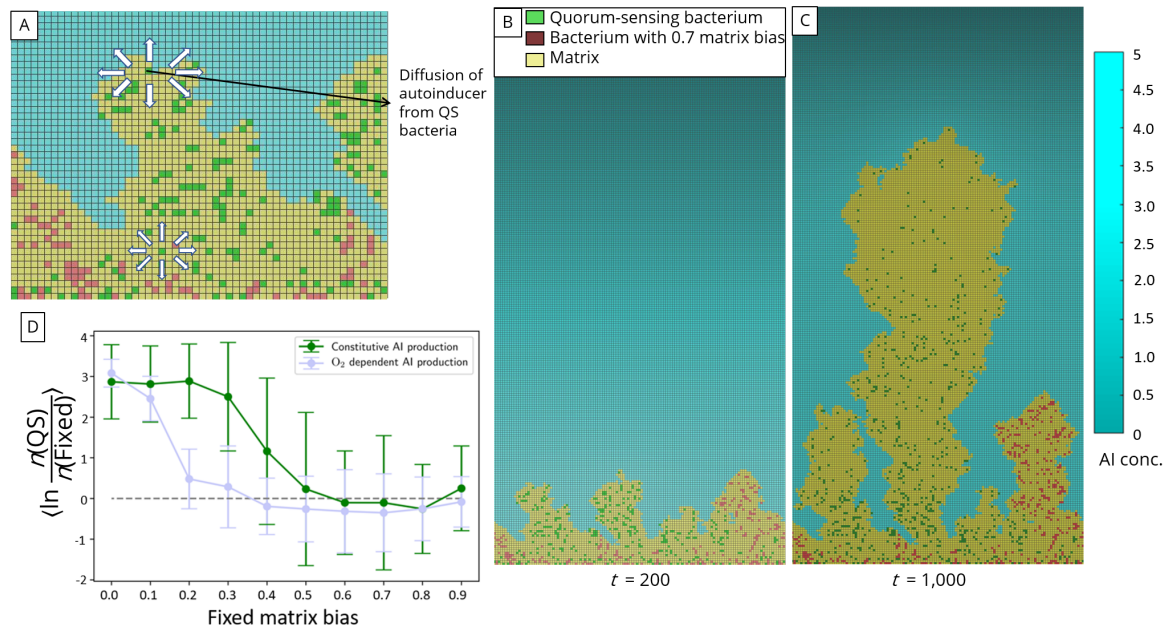


Fig. 3. Simulated biofilm competitions between nutrient-limited QS cells that produce AI proportional to local O_2 concentration and non-QS cells. (A) QS cells shown in green produce AI at a rate proportional to local O_2 concentration (arrows highlight AI diffusion). Bacterial cells shown in red do not produce any AI. (B) Snapshot of a pairwise competition after 200 simulation timesteps. Green QS cells adjust their matrix bias based on local AI concentration as in Fig. 2. Red cells do not produce AI and have a fixed matrix bias of 0.7. Shade of squares indicates local AI concentration (in arbitrary units as described in the *SI Appendix*, and O_2 diffuses from above. (C) Snapshot of the same competition in B after 1,000 timesteps. (D) Mean of the natural logarithm of the final ratio of number of O_2 -dependent QS cells to number of fixed-strategy cells. The error bars indicate standard deviations of log ratios. Over 60 simulations were performed for each competition.

166 the case of constitutive AI production where the total AI
167 production and concentration both increase with the total
168 population of QS bacteria.

169 **A Novel Biophysical Limit.** In our simple 2D simulations we
170 found that nutrient-limited QS strategies provided little or
171 no benefit to cells competing for a diffusible resource. Does
172 this conclusion apply in more realistic settings? Perhaps
173 surprisingly, we found that the answer is yes: There exists a
174 corresponding biophysical limit for the efficacy of QS in 3D
175 for bacteria whose AI production is limited by uptake of a
176 diffusible nutrient (derivation in *SI Appendix*). Specifically,
177 there is an upper limit on the dynamic range, DR, of possible
178 AI concentrations experienced by cells for a given source of
179 diffusible nutrient. For a diffusible, non-decaying AI, the
180 minimum AI concentration, $[AI]_{\min}$, is that experienced by a
181 single isolated cell, which senses only its own AI production.
182 We prove that no matter how cells are arranged in 3D, the
183 maximum AI concentration that any cell can experience has
184 an upper bound specified by

$$185 \quad DR \equiv \frac{[AI]_{\max}}{[AI]_{\min}} = \frac{4\pi D_{O_2} r_0}{\gamma} + 1, \quad [2]$$

186 where D_{O_2} is the diffusion constant for O_2 (which we take
187 to be the limiting nutrient), r_0 is the cell radius, and γ is
188 the rate of intake of O_2 per cell per concentration of O_2 .
189 Intuitively, the biophysical limit expressed by Eq. 2 comes from
190 recognizing that in and around a biofilm the O_2 concentration
191 and AI concentration are effectively mirror images. This
192 follows because O_2 is linearly converted to AI, so local O_2
193 consumption translates to local AI production, and both O_2
194 and AI satisfy corresponding diffusion equations. This means

195 that the local AI concentration can never be higher than a
196 limit set by the minimum local O_2 concentration, which is
197 zero. Since a single isolated cell already experiences a finite AI
198 concentration due to its own AI production, this upper limit
199 on AI concentration implies an absolute upper bound on the
200 dynamic range DR.

201 Under what conditions can DR be large? Intuitively, large
202 DR requires a small $[AI]_{\min}$ so a cell on its own must be a
203 relatively weak producer of AI, i.e. it must be a weak
204 consumer of O_2 . Indeed, the combination of parameters $D_{O_2} r_0 / \gamma$
205 in Eq. 2 is large if a single cell only weakly perturbs the local
206 O_2 concentration, by a combination of large values of D_{O_2} and
207 r_0 and a small uptake rate γ , which implies fast replenish-
208 ment of local O_2 by diffusion. But these conditions are not
209 consistent with a narrow growth layer, which is precisely the
210 case for which modeling studies have found an advantage for
211 QS-mediated matrix production.

212 What then does the biophysical limit on the DR of AI
213 concentrations imply for the efficacy of QS as a regulator of
214 matrix production in biofilms? To answer this question, note
215 that the penetration depth of a limiting nutrient, say O_2 , into
216 a biofilm is $\lambda = \sqrt{D_{O_2} / \gamma \rho}$, where ρ is the local cell density.
217 The limit on AI dynamic range can therefore be rewritten as

$$218 \quad DR = 4\pi \rho \lambda^2 r_0 + 1. \quad [3] \quad 219$$

219 To estimate this DR, a typical bacterial cell has a radius of
220 approximately $1 \mu\text{m}$ (24), typical cell densities of bacteria are
221 around 5×10^8 cells/ml for *Escherichia coli* in biofilms (25),
222 and the O_2 penetration depth for *Pseudomonas aeruginosa*
223 was found by microelectrode studies (26) to be $30 \mu\text{m}$. For
224 these values, we obtain the DR to be approximately 6. We

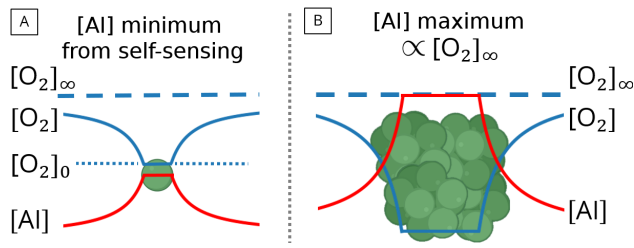


Fig. 4. Schematic illustrating the limited dynamic range of AI concentrations. (A) A single bacterial cell, consuming oxygen and secreting AI. The AI concentration in the vicinity of the cell is proportional to the difference between the O_2 concentration at infinity, $[O_2]_\infty$, and the O_2 concentration in the vicinity of the cell, $[O_2]_0$. (B) A bacterial colony, consuming O_2 and secreting AI. If the O_2 concentration inside the colony is close to zero, the AI concentration approaches a maximum value $\propto [O_2]_\infty$. This relation between the AI concentration and O_2 concentration leads to the upper limit on the dynamic range of AI described in Eqs. 2 and 3.

the minimum AI concentration in the case of decaying AI may be arbitrary low for a cell deep in a biofilm where all AI is produced at the boundary and decays before reaching the deep interior. However, such a reduction of AI concentration is irrelevant to the growth strategy, since cells deep in the interior are nutrient-starved and so cannot produce substantial biomass.)

Our main conclusion is that for bacterial cells to reliably infer local cell density via quorum sensing, AI production must not be metabolically slaved. We believe that despite the strong links between metabolism and AI production (15, 16, 32, 33), and the substantial cost of AI production (34, 35), cells are able to decouple the two processes and regulate AI production largely independent of cell metabolism. This is consistent with the prevailing understanding in the literature that cells use cheap AI signals to assess the efficacy of costlier cooperative behaviors (36). Thus, we identify AI production and quorum sensing as a privileged bacterial function that is prioritized by bacteria, even when a lack of nutrients limits other functions.

Materials and Methods

All simulations were performed via agent-based modeling using Nanoverse (18). At each timestep, the reaction-diffusion equations for the O_2 and AI concentrations specified by their production, consumption, and decay (if any) are solved to obtain their steady-state concentrations. This steady-state concentration determines the matrix production strategy and the probabilities in each timestep of matrix production and/or reproduction. If a cell produces matrix and/or reproduces in a timestep, then the positions of some surrounding matrix and bacterial cells are "shoved" as necessary to allow the newly produced matrix/cell to occupy a lattice site adjacent to the cell that produced it. After all matrix production and reproduction has taken place, the reaction-diffusion equations are again solved for the next timestep. This alternating procedure is repeated until the simulation halts at a pre-specified halt condition. For additional details, see *SI Appendix*.

ACKNOWLEDGMENTS. We thank Bonnie Bassler, Farzan Beroz, Daniel Greenidge, Matthew Jemielietta, Ameya Mashruwala, Yigal Meir, and Jing Yan for stimulating discussions and input. A.V.N. acknowledges support from the Princeton University Physics Department, Office of the Dean of Research at Princeton University, UCSD Physics Department, and the qBio program at UCSD. This research was supported, in part, by National Institutes of Health Grant R01-GM082938 (to N.S.W.). This work was supported in part by the National Science Foundation, through the Center for the Physics of Biological Function (PHY-1734030). This work was done on land considered part of the ancient homelands of the Lenni-Lenape and the Kumeyaay peoples.

1. HC Flemming, J Wingender, The biofilm matrix. *Nat. Rev. Microbiol.* **8**, 623–633 (2010).
2. JS Dickschat, Quorum sensing and bacterial biofilms. *Nat. Prod. Reports* **27**, 343–369 (2010).
3. YH Li, X Tian, Quorum sensing and bacterial social interactions in biofilms. *Sensors* **12**, 2519–2538 (2012).
4. MR Parsek, EP Greenberg, Sociomicrobiology: the connections between quorum sensing and biofilms. *Trends Microbiol.* **13**, 27–33 (2005).
5. C Solano, M Echeverez, I Lasa, Biofilm dispersion and quorum sensing. *Curr. Opin. Microbiol.* **18**, 96–104 (2014).
6. S Remuzgo-Martínez, et al., Biofilm formation and quorum-sensing-molecule production by clinical isolates of *Serratia liquefaciens*. *Appl. Environ. Microbiol.* **81**, 3306–3315 (2015).
7. ST Rutherford, BL Bassler, Bacterial quorum sensing: its role in virulence and possibilities for its control. *Cold Spring Harb. Perspectives Medicine* **2**, a012427 (2012).
8. DG Davies, et al., The involvement of cell-to-cell signals in the development of a bacterial biofilm. *Science* **280**, 295–298 (1998).
9. JB Xavier, KR Foster, Cooperation and conflict in microbial biofilms. *Proc. Natl. Acad. Sci.* **104**, 876–881 (2007).
10. CD Nadell, JB Xavier, SA Levin, KR Foster, The evolution of quorum sensing in bacterial biofilms. *PLoS Biol* **6**, e14 (2008).

stress that Eq. 3 is the *theoretical upper bound* for the dynamic range in such a system, and in real biological settings, the actual value may be lower. Indeed, the DR is smallest when the limiting nutrient is most efficiently taken up by the outermost layers of cells, i.e. for a narrow active growth layer.

Discussion. We find that when production of a non-decaying AI is limited by a diffusible nutrient from a remote source, there exists a biophysical limit on the dynamic range of AI concentrations that cells can experience. Using agent-based simulations of biofilm growth, we demonstrate an illustrative case in which QS-based matrix-production strategies can provide a large competitive advantage— but not if AI production is limited by nutrient availability. Importantly, the biophysical limit is independent of the diffusivity of the autoinducer. Further, the result is essentially independent of the size, shape, or detailed distribution of cells, or of the diffusion rate of the growth-limiting nutrient.

In principle, nutrient-limited AI production could still be exploited by bacteria in several ways. For example, in a biofilm where the density of cells is high, bacteria could employ QS to infer the concentration of the diffusible nutrient at its source. This is because, for a non-decaying AI, the local AI concentration mirrors the nutrient concentration, so that locally depleted nutrient but a high AI concentration would imply a large nutrient source. Further, even at lower cell densities, nutrient-limited AI could act as a single consolidated chemotactic signal that would indicate, via its gradient, the direction of the source of the currently growth-limiting nutrient.

Autoinduction, i.e. positive feedback of AI production from AI sensing is a well-established feature of many quorum-sensing systems (27–31). However, it is not fully understood why autoinduction per se is necessary for cells to sense their local density. It could be presumed that a higher density of cells would necessarily result in a higher AI concentration, obviating the need for positive feedback on AI production. However, this presumption would not be correct if AI production were nutrient limited – above a threshold cell density AI concentration would hit its maximum, and provide no further information. From this perspective, autoinduction may simply represent one way of breaking the dependence of AI production on nutrient availability, in order to evade the biophysical limit on the dynamic range of AI concentrations (Eqs. 2 and 3). (We note that our derivation is for non-decaying AI, and

- 334 11. JA Fozard, M Lees, JR King, BS Logan, Inhibition of quorum sensing in a computational
335 biofilm simulation. *Biosystems* **109**, 105–114 (2012).
- 336 12. P Melke, P Sahlin, A Levchenko, H Jönsson, A cell-based model for quorum sensing in
337 heterogeneous bacterial colonies. *PLoS Comput. Biol.* **6**, e1000819 (2010).
- 338 13. M Lees, B Logan, J King, Hla simulation of agent-based bacterial models in *European Simu-*
339 *lation Interoperability Workshop*. (2007).
- 340 14. M Lees, B Logan, J King, Multiscale models of bacterial populations in *Proceedings of the*
341 *39th Conference on Winter Simulation: 40 years! The best is yet to come*. (IEEE Press), pp.
342 881–890 (2007).
- 343 15. MR Parsek, DL Val, BL Hanzelka, JE Cronan, EP Greenberg, Acyl homoserine-lactone
344 quorum-sensing signal generation. *Proc. Natl. Acad. Sci.* **96**, 4360–4365 (1999).
- 345 16. MI Moré, LD Finger, JL Stryker, et al., Enzymatic synthesis of a quorum-sensing autoinducer
346 through use of defined substrates. *Science* **272**, 1655 (1996).
- 347 17. W Ding, et al., s-adenosylmethionine levels govern innate immunity through distinct
348 methylation-dependent pathways. *Cell Metab.* **22**, 633–645 (2015).
- 349 18. DB Borenstein, Ph.D. thesis (Princeton University) (2015).
- 350 19. PS Stewart, Diffusion in biofilms. *J. Bacteriol.* **185**, 1485–1491 (2003).
- 351 20. D De Beer, P Stoodley, F Roe, Z Lewandowski, Effects of biofilm structures on oxygen distri-
352 bution and mass transport. *Biotechnol. Bioeng.* **43**, 1131–1138 (1994).
- 353 21. PS Stewart, Mini-review: convection around biofilms. *Biofouling* **28**, 187–198 (2012).
- 354 22. J Yan, CD Nadell, BL Bassler, Environmental fluctuation governs selection for plasticity in
355 biofilm production. *The ISME J.* **11**, 1569 (2017).
- 356 23. JB Xavier, C Picioreanu, MC Van Loosdrecht, A framework for multidimensional modelling of
357 activity and structure of multispecies biofilms. *Environ. Microbiol.* **7**, 1085–1103 (2005).
- 358 24. H Kubitschek, J Friske, Determination of bacterial cell volume with the coulter counter. *J.*
359 *Bacteriol.* **168**, 1466–1467 (1986).
- 360 25. MG Surette, BL Bassler, Quorum sensing in escherichia coli and salmonella typhimurium.
361 *Proc. Natl. Acad. Sci.* **95**, 7046–7050 (1998).
- 362 26. KD Xu, PS Stewart, F Xia, CT Huang, GA McFeters, Spatial physiological heterogeneity in
363 pseudomonas aeruginosa biofilm is determined by oxygen availability. *Appl. Environ. Micro-*
364 *biol.* **64**, 4035–4039 (1998).
- 365 27. KH Nealon, Autoinduction of bacterial luciferase. *Arch. Microbiol.* **112**, 73–79 (1977).
- 366 28. CM Waters, BL Bassler, Quorum sensing: cell-to-cell communication in bacteria. *Annu. Rev.*
367 *Cell Dev. Biol.* **21**, 319–346 (2005).
- 368 29. MB Miller, BL Bassler, Quorum sensing in bacteria. *Annu. Rev. Microbiol.* **55**, 165–199
369 (2001).
- 370 30. WL Ng, BL Bassler, Bacterial quorum-sensing network architectures. *Annu. Rev. Genet.* **43**,
371 197–222 (2009).
- 372 31. K Papenfort, BL Bassler, Quorum sensing signal–response systems in gram-negative bacte-
373 ria. *Nat. Rev. Microbiol.* **14**, 576 (2016).
- 374 32. K Papenfort, et al., A *Vibrio cholerae* autoinducer–receptor pair that controls biofilm formation.
375 *Nat. Chem. Biol.* **13**, 551–557 (2017).
- 376 33. S Schauder, K Shokat, MG Surette, BL Bassler, The luxs family of bacterial autoinducers:
377 biosynthesis of a novel quorum-sensing signal molecule. *Mol. Microbiol.* **41**, 463–476 (2001).
- 378 34. L Keller, MG Surette, Communication in bacteria: an ecological and evolutionary perspective.
379 *Nat. Rev. Microbiol.* **4**, 249–258 (2006).
- 380 35. A Ruparell, et al., The fitness burden imposed by synthesising quorum sensing signals. *Sci.*
381 *Reports* **6**, 33101 (2016).
- 382 36. BA Hense, M Schuster, Core principles of bacterial autoinducer systems. *Microbiol. Mol. Biol.*
383 *Rev.* **79**, 153–169 (2015).